Cell Biochemistry and Biophysics (2019) 77:319–333
https://doi.org/10.1007/s12013-019-00887-0

ORIGINAL PAPER

Check for updates

Multi-Dimensional Screening Strategy for Drug Repurposing with Statistical Framework—A New Road to Influenza Drug discovery

K. Rohini[1] · K. Ramanathan[1] · V. Shanthi[1]

Received: 6 April 2019 / Accepted: 16 September 2019 / Published online: 26 September 2019

Abstract

Influenza virus is known for its intermittent outbreaks affecting billions of people worldwide. Several neuraminidase inhibitors have been used in practice to overcome this situation. However, advent of new resistant mutants has limited its clinical utilization. In the recent years drug repurposing technique has attained the limelight as it is cost effective and reduces the time consumed for drug discovery. Here, we present multi-dimensional repurposing strategy that integrates the results of ligand-, energy-, receptor cavity, and shape-based pharmacophore algorithm to effectively identify novel drug candidate for influenza. The pharmacophore hypotheses were generated by utilizing the PHASE module of Schrödinger. The generated hypotheses such as AADP, AADDD, and DDRRNH, respectively, for ligand-, e-pharmacophore and receptor cavity based approach alongside shape of oseltamivir were successfully utilized to screen the DrugBank database. Subsequently, these models were evaluated for their differentiating ability using Enrichment calculation. Receiver operating curve and enrichment factors from the analysis indicate that the models possess better capability to screen actives from decoy set of molecules. Eventually, the hits retrieved from different hypotheses were subjected to molecular docking using Glide module of Schrödinger Suite. The results of different algorithms were then combined to eliminate false positive hits and to demonstrate reliable prediction performance than existing approaches. Of note, Pearson's correlation coefficients were calculated to examine the extent of correlation between the glide score and IC50 values. Further, the interaction profile, pharmacokinetic, and pharmacodynamics properties were analyzed for the hit compounds. The results from our analysis showed that alprostadil (DB00770) exhibits better binding affinity toward NA protein than the existing drug molecules. The biological activity of the hit was also predicted using PASS algorithm that renders the antiviral activity of the compound. Further, the results were validated using mutation analysis and molecular dynamic simulation studies. Indeed, this integrative filtering is able to exceed accuracy of other state-of-the-art methods for the drug discovery.

Keywords Neuraminidase · Pharmacophore Model · Oseltamivir · Enrichment Calculation · Virtual Screening · Molecular Docking · Molecular Dynamic Simulation

Abbreviations

NA	Neuraminidase
PDB	Protein Data Bank
CPH	Common pharmacophore hypothesis
EF	Enrichment factor
ROC	Receiver Operating Curve
HTVS	High-throughput virtual screening
SP	Standard precision
XP	Extra precision
MD	Molecular Dynamics
OPLS	Optimized Potentials for Liquid Simulations
DUD	Directory of Useful Decoys
CNS	Central nervous system
DHEA	Dehydroepiandrosterone
SMARTS	SMiles ARbitary Target Specification
RMSD	Root Mean Square Deviations
RMSF	Root Mean Square Fluctuations
ADME	Absorption, Distribution, Metabolism and Excretion

✉ V. Shanthi
shanthi.v@vit.ac.in

[1] Department of Biotechnology, School of Bio Sciences and Technology, Vellore Institute of Technology, Vellore, Tamil Nadu 632014, India

Introduction

Influenza infection endures to be a substantial health concern worldwide and the advent of several pandemics has

become a constant menace. It is reckoned that over 60 million individuals fell ill with 2009 pandemic H1N1 in USA in the year 2009 and 2010. In addition, more than 12,000 deaths were related to H1N1 infection in the same flu season [1]. The emergence of such pandemics and epidemics is due to unpredictable mutations in the proteins of influenza A virus. Most importantly, the surface glycoprotein, neuraminidase (NA), is subjected to such fatal mutations [2]. The NA protein is believed to play crucial roles in influenza virus lifecycle [3]. It aids in the facilitation of viral proliferation by cleaving the terminal sialic acid residue. Therefore, this enzyme has been considered as an attractive target for antiviral therapy [4]. The widely used NA inhibitors (NAIs) for influenza treatment are oseltamivir and zanamivir [5]. However these drugs are entirely different in the method of administration, pharmacological effect, and their side effects. In particular, inhalation is the preferred method for zanamivir as it has a poor oral availability. Oseltamivir on the other hand possesses good oral availability and thus is preferred as best antiviral drug for the treatment of influenza [6]. In addition, two novel NAIs, peramivir and laninamivir, were approved in the year 2010 to treat influenza infection [7]. However, clinical application of NAIs remains restricted due to the emergence of drug-resistant mutants. Some of the most prevalent mutations are H274Y, R292K, N294S, I221L, I223R, and H275Y [8–12]. Thus, this situation necessitates developing novel NAIs with alternate binding pattern to overcome resistance.

De novo drug discovery process has become time-consuming and tedious over the last few years. Despite of the increased investments in the pharmaceutical research and development centers, the number of approvals for new drugs has declined [13]. In view of these challenges, drug repurposing has emerged as a boon that aids in the identification and development of new indications for existing drugs in market. This strategy could essentially reduce the developmental cost and the time frame required to discover a novel drug [14]. For instance, the successful repositioned drugs such as thalidomide, raloxifene, and sildenafil have generated high revenue for their patent holders. In the recent era, several computational methods including structure based and pharmacophore-based screening have unlocked the way for cost effective and quick designing and development of drugs [15, 16].

In the race to discover a more efficacious NAI, molecular docking has been an extremely beneficial tool utilized by researchers to expedite the exacting process. However, we need to use other computational methods before we attempt to dock a compound to a target protein to reduce the docking load. For instance, pharmacophore is the essential to understand the interaction between the receptor and ligand. It is an important feature to design new drug for treatment of the intended disease. Other methods such as e-pharmacophore and receptor cavity based models can be used prior to the molecular docking to reduce computational load and time [17–20]. But its ability to screen a viable candidate is still generally questioned. Therefore, the present study aimed to identify a potent inhibitor against NA protein by integrating available pharmacophore-based screening strategies such as Ligand-, e-Pharamacophore-, Receptor cavity-, and Shape-based screening in the initial stage. Therefore in the current study, we have attempted to identify potent NAIs by using novel prediction method, which adopts different algorithms to demonstrate better prediction accuracy.

Materials and Methods

Preparation of Dataset

The three-dimensional structure of the protein was extracted from Protein Data Bank database (PDB) [21], with the identification number 3TI6 having a resolution of 1.69 Å [22]. In addition, the NA mutant structures such as 4HZZ (H274Y), 1L7H (R292K), 1L7G (E119G), 3CL2 (N294S), 4B7N (I223R), 3K39 (D179E), and 4CPM (I221L) were also retrieved. The ligands comprise of a combination of FDA approved drugs (oseltamivir, zanamivir, laninamivir, and peramivir) and few investigational drugs (MK2206, crenatoside, dehydroepiandrosterone (DHEA), and tamiphosphor) (Fig. 1). The two-dimensional structures of these drug molecules were retrieved from PubChem library maintained by NCBI. Lastly, the FDA-approved assortment of DrugBank database consisting of 2037 molecules is used for the virtual screening processes.

Ligand Preparation

The ligands used in our analysis were prepared using LigPrep module of Schrödinger Suite. It is widely used for the energy minimization of small molecules. The ligands are prepared using the Optimized Potentials for Liquid Simulations (OPLS)-2005 force field at physiological pH of 7 [23]. Initially, the protonation states of ligands were assigned and the torsions were modified. Moreover, the preparation also included generation of stereoisomer, detection of possible ionization state, and attachment of hydrogen molecules [24]. These prepared ligands were used in the screening processes.

Protein Preparation

The necessary protein preparation for our analysis was performed automatically by launching the Protein

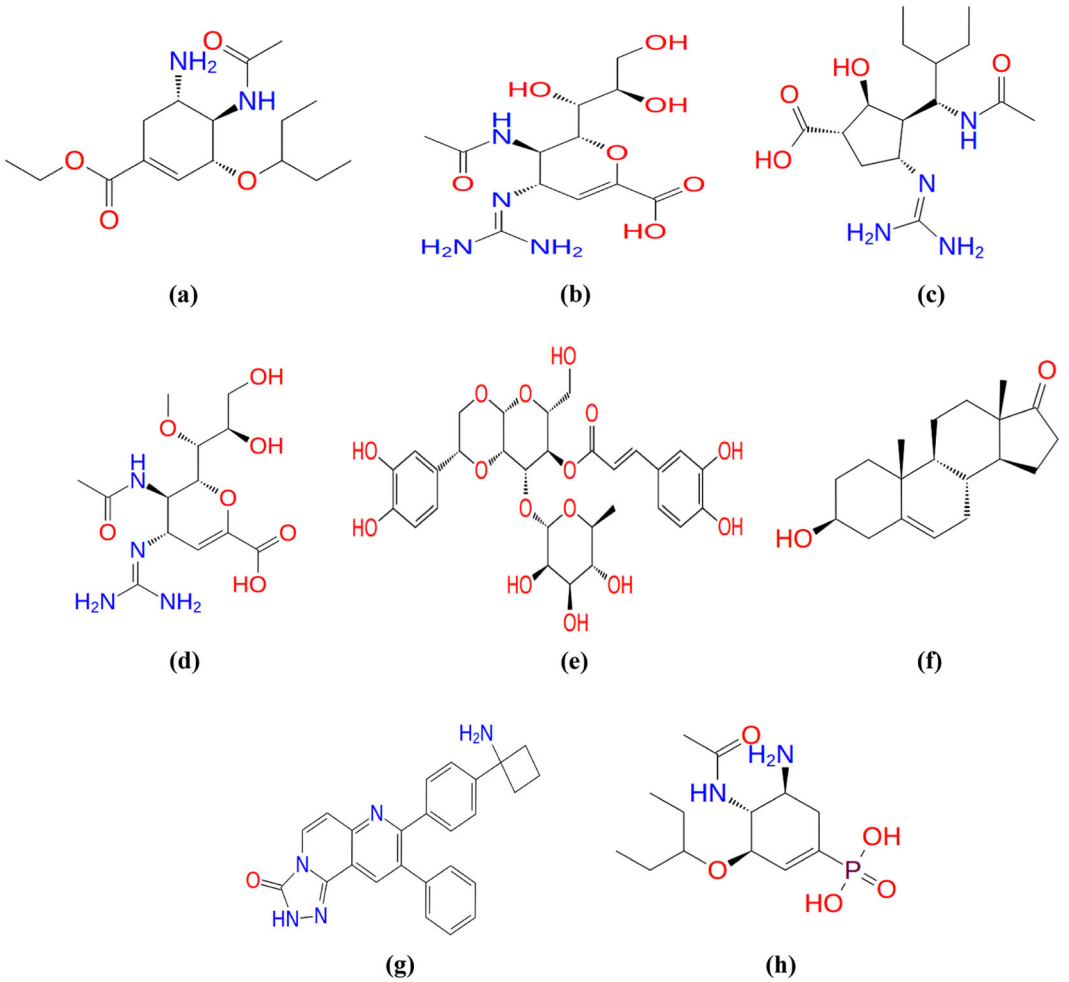

Fig. 1 2D structure illustration of **a** oseltamivir, **b** zanamivir, **c** peramivir, **d** laninamivir, **e** crenatoside, **f** DHEA, **g** MK2206, and **h** tamiphosphor

Preparation Wizard of Schrodinger Suite. This tool helps in rectifying the structural defects existing in the protein structure. Some of the typical operations include (i) addition of hydrogen atoms, (ii) assignment atomic charges, and (iii) elimination of water molecules that are not involved in ligand binding etc. Initially, the protein was pre-processed and water molecules were removed up to a distance of 5.0 Å. Subsequently, right bond orders were assigned and the heteroatoms that do not affect the conformation of protein were deleted. Further, H-atoms were appended to the carbon atoms. Then, structure optimization and minimization step were carried out using OPLS-2005 force field. Finally the protein structure was subjected to restrained minimization with a RMSD (Root Mean Square Deviation) value of 0.30 Å [25].

Multi-Dimensional Pharmacophore Hypothesis

In the present study, the PHASE algorithm implemented in Schrödinger package was used to generate a ligand-, energy-, receptor cavity-, and shape-based pharmacophore hypothesis. Although utilizing pharmacophoric features has proven useful (and has been widely applied), they may be not adequate for a risk-sensitive drug discovery application. Thus, we planned to integrate these methods alongside statistical validation to explore the polypharmacology effects of drug compounds.

Ligand-based Pharmacophore Modeling

The ligand-based pharmacophore hypothesis generated using the set of known FDA approved and investigational NAIs. PHASE module is a multifaceted tool for structure alignment, pharmacophore modeling, and 3D database screening. It utilizes a tree-based partitioning algorithm to determine a common pharmacophore hypothesis (CPH) [26]. These hypotheses represent the attributes of 3D chemical structures that play vital role in binding. Initially, Confgen was used to generate the conformers for each ligands by utilizing OPLS-2005 force field [27]. A set of

SMiles ARbitary Target Specification patterns that define the six inbuilt pharmacophoric features viz. hydrogen bond donor (D), hydrogen bond acceptor (A), aromatic ring (R), hydrophobic group (H), negatively ionizable group (N), and positively ionizable group (P) were considered for model generation [28]. A CPH was generated from active ligands of the dataset, utilizing these features. Before the generation of CPH, a list of hypotheses is subjected to rigorous scoring process. It will score the hypotheses on the basis of vector score, alignment score, and volume score of active ligands with the corresponding hypotheses. Eventually, the PHASE provides both survival active and inactive scores for all the hypotheses. In particular, it has been reported that hypotheses with higher survival inactive scores can effectively discriminate between inactive and active ligands [28]. Thus, the hypothesis with maximum survival inactive score was selected to screen the FDA approved set of DrugBank database.

E-Pharmacophore-Based Virtual Screening

The e-pharmacophore method generates a pharmacophore model by taking the docked pose of complexes as input. The resultant e-pharmacophore model examines for the intrinsic flexibility and ease of ligands to bind with the active site efficiently [29]. Initially, "Receptor grid generation" tool in Glide module of Schrödinger Suite was utilized to generate a receptor grid within a cubic box focused on crystallized inhibitor. Subsequently, the XP (extra precision) docking was performed using Glide package through the generated grid [30]. Ultimately, the model was formed employing the six inbuilt pharmacophoric features present in PHASE module. Each pharmacophoric feature obtained was labeled with particular energy value equal to the sum of Glide XP contributions of all atoms present in the site. This helps in examining and arranging the sites with respect to energy values. Finally, on the basis of the Glide XP energies of pharmacophoric features, the best e-pharmacophore model was selected for virtual screening.

Receptor Cavity Based Virtual Screening

The receptor cavity based virtual screening is a flexible and powerful method, used to screen potent inhibitors for orphan receptors. This method involves consideration of chemical features of the binding pocket residues of the target protein [19]. Initially, the binding pocket residues of the target are determined using SiteMap module of Maestro package [31]. The PHASE module employs a multiple copy simultaneous search method to find energetically favorable positions and properties of molecules to generate a receptor cavity based pharmacophore model [19]. Subsequently, resultant residues from SiteMap analysis were used as an input to generate the model. Finally, it was used to screen large databases to obtain potent inhibitors for the receptor.

Shape Screening Method

Shape-based screening method has proven to be valuable in the field of in silico drug design. This method is developed from the idea that molecules with similar shapes exhibiting similar biological activity. The chemical features of the ligand molecule are quantitatively compared with the compounds of a database [20]. In this method each conformer of the database molecule is aligned to the reference ligand and a similarity was calculated based on the overlapping of hard sphere volumes. The molecule exhibiting highest similarity score was taken for further analysis. In all our investigation, oseltamivir was considered as the reference ligand.

Enrichment Calculation

Prior to virtual screening procedure, the differentiating ability of the pharmacophore models was evaluated using the "Enrichment calculator" tool of Schrödinger Suite. The decoy set corresponding to influenza NA was extracted from library of Directory of Useful Decoys [32]. The set consists of 1882 compounds, inclusive of 1874 decoys and eight known ligands, were utilized to introspect the integrity of the models. The parameters such as enrichment factor (EF) and receiver operating characteristics curve value (ROC) were analyzed. The EF value highlights the recovery rate of true positives from the decoy set, while ROC value focuses on the relationship between true positives (sensitivity) and false positives (1-specificity) [33].

Molecular Docking

Molecular docking experiment for all the screened compounds with NA was performed using Glide of Schrödinger to calculate the binding affinity of the compounds. It has been successfully used in various studies to discover potent inhibitors and filter out those compounds that do not bind efficiently to the target protein [17, 34]. Initially, the extend of correlation between glide docking algorithm and IC50 was analyzed through Pearson's correlation coefficient with the help of 12 NAIs retrieved from the literature. Subsequently, three stage docking procedure was used that includes, high-throughput virtual screening (HTVS), standard precision (SP), and XP mode to explore the hits.

Note that ConfGen tool implemented in the Glide was used to generate the ligand conformers independent of the receptor/grid in the initial stage. Each conformer is then docked into the binding pocket via molecular, rotational, and translation motions. Further, OPLS force field was utilized to execute a complete systematic search of the conformational, orientational, and positional space of the docked ligand. Finally, the best conformation is selected based on torsion energies and are eventually docked into protein binding sites with soft potentials [30]. The shape and properties of the binding site are depicted on the receptor grid, which gradually devises a more accurate scoring of ligand pose. This progressive process ultimately searches for constructive interactions between protein and the ligands [35]. Finally, the best hits retaining favorable interactions and better docking scores than known inhibitors were acquired.

In silico Prediction of Absorption, Distribution, Metabolism and Excretion (ADME) Properties

Here, Qikprop program [36] was used to introspect the ADME properties of the resultant hits. It evaluates 49 pharmaceutically relevant descriptors and provides range to contrast with the properties of 95% known drugs. In the current study, the values of descriptors such as QPlogKp, QPlogBB, QPlogS, QPlogPo/w, QPlogPw, central nervous system (CNS), #stars, and QPlogPoct were compared with the known NAIs values. In particular the #stars and CNS values, respectively, signify the number of violations and activity of molecule against CNS. For instance, lower values of #stars and negative CNS implies the more drug-like CNS inactive molecule.

PASS Prediction Algorithm and Mutation Studies

The biological activity of hit compound was examined using PASS algorithm [37]. It efficiently predicts 4130 types of biological activity with 95% mean prediction accuracy. The smiles format of each of the hit compound is provided as the input for the PASS prediction. Subsequently, the results are obtained as a list of predicted biological activity along with its Pa (Active probability) and Pi (Inactive probability) values. In addition, to resolve the problem of drug resistance, the hit compound was further docked with NA mutant structures to analyse its efficacy towards experimentally proven mutants using XP docking algorithm.

Molecular Dynamic (MD) Simulation

The MD simulation was executed using the GROMACS v.4.6.3 with the force field of GROMOS43a1 [38]. MD simulation analyses have been extensively employed to gain insight into the structural stability and dynamic behavior of docked complexes with time. Thus, in the current study, MD simulation was performed to interpret the binding efficacy of hit compound against the NA protein. The procured information was further mapped to the NA-oseltamivir complex file to unravel the complex stability and affinity.

Initially, the topology files for ligands were generated with the PRODRG server [39]. The docked structures were solvated in SPC (simple point charge) water molecules inside a 0.9-nm periodic cubic box. The solvated system was then neutralized by adding three positive counter ions. After the solvation process, the system was energy minimized using the GROMOS43a1 force field. Subsequently, the minimized system was then subjected to 50 ns simulation at constant temperature (300 K) (NVT) and pressure (1.01325 bar) (NPT) [40]. The trajectories were retrieved for every 1 ps for the structural analysis. The parameters such as RMSD, root mean square fluctuations (RMSF), and number of inter hydrogen bonds were calculated through GROMACS utilities g_rms, g_rmsf and g_hbond, respectively. In addition, clustering analysis with a RMSD cut-off of 0.125 nm was also performed using the g_cluster utility implemented in GROMACS. Furthermore, the binding pockets of each complex at various time frames were also analysed using SiteMap module of Schrödinger suite.

Results and Discussion

Ligand-Based Pharmacophore Hypothesis

In ligand-based approach, the dataset was initially divided into active and inactive molecules to generate the hypothesis. The FDA approved set of inhibitors were considered as the actives while the investigational drug molecules were considered as inactives. Further the generated hypotheses were scored by applying the scoring function. The hypothesis with topmost survival active and survival inactive scores were utilized for screening the database. For instance, the best model obtained consisted of two hydrogen bond acceptors (A), one hydrogen bond donor (D), and one positively charged group (P), AADP, (Fig. 2a) with a survival active and inactive score of 3.921 and 3.814, respectively.

E-Pharmacophore Model Generation

Unlike the ligand-based strategy, the Glide XP docked structures of protein complexes were taken as an input to generate a pharmacophore model. The e-pharmacophore

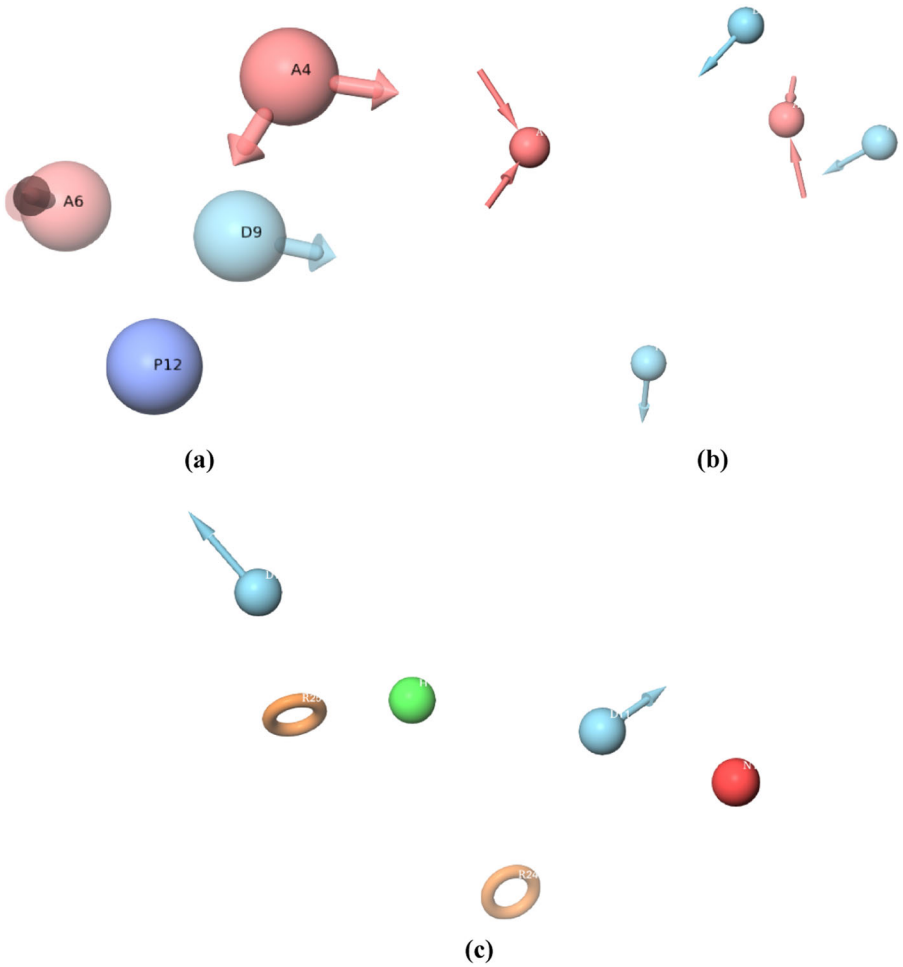

Fig. 2 Pharmacophore hypotheses generated for **(a)** ligand based pharmacophore model; four—featured pharmacophore hypothesis with two hydrogen bond acceptors (A; red), one hydrogen bond donor (D; light blue), and one positively charged group (P; dark blue) **b** e-pharmacophore model; five-featured pharmacophore hypothesis with three hydrogen bond donors (D; light blue) and two hydrogen bond acceptors (A; red) and **c** receptor cavity based pharmacophore model; six-feature pharmacophore hypothesis with two aromatic rings (R; orange), two hydrogen bond donors (D; light blue), one hydrophobic group (H; green), and one negatively charged group (N; red)

hypothesis was built by mapping energetic terms of Glide XP on pharmacophoric features. These energetic terms were computed using the structural and energy information present in between the protein and ligand molecule [41]. Subsequently a five featured pharmacophore was developed that consists of two hydrogen bond acceptors (A) and three hydrogen bond donors (D), AADDD (Fig. 2b). Moreover, in the process of model generation it was also assured that the features should possess an energy score greater than −0.8 kcal/mol, which was set as a threshold. This helps to prioritize the vital sites responsible for efficient binding.

Receptor Cavity Based Virtual Screening

Here, the binding site residues of the protein were determined by SiteMap tool. The amino acid residues that constituted the binding pocket of NA protein includes R 118, E 119, L 134, D 151, R 152, R 156, W 178, S 179, D 198, N 221, I 222, R 224, E 227, S 246, H 274, E 276, E 277, R 292, N 294, N 347, R 371, Y 406, and E 425 were considered. Moreover, the receptor binding site of the native protein was defined by the 3D coordinates of the centroid of active site. For instance, X, Y, and Z coordinates of centroid were set as −28.75, 14.72, and 20.33, respectively. Subsequently, a six featured pharmacophore hypothesis was generated consisting of 2D, 2 R, 1 N, and 1 H group (DDRRNH) (Fig. 2c).

Enrichment Analysis

Prior to screening, all the three generated hypothesis were examined for its discriminating power to sift the active ligands from a decoy set. Enrichment calculator tool of Schrödinger Suite was used to perform the hypothesis validation. The EF (1%) value of 99 and 98 for ligand based and e-pharmacophore model, respectively, depicts the highest recovery of true active ligands from the decoy set. On the contrary, receptor cavity based pharmacophore model, yielded a lower EF value of 76. In addition, ROC parameters for the models were also calculated. The ROC plots for the models are represented in Fig. 3. It is clear from the figure that ROC curves for both ligand and e-pharmacophore-based model initially extends vertically.

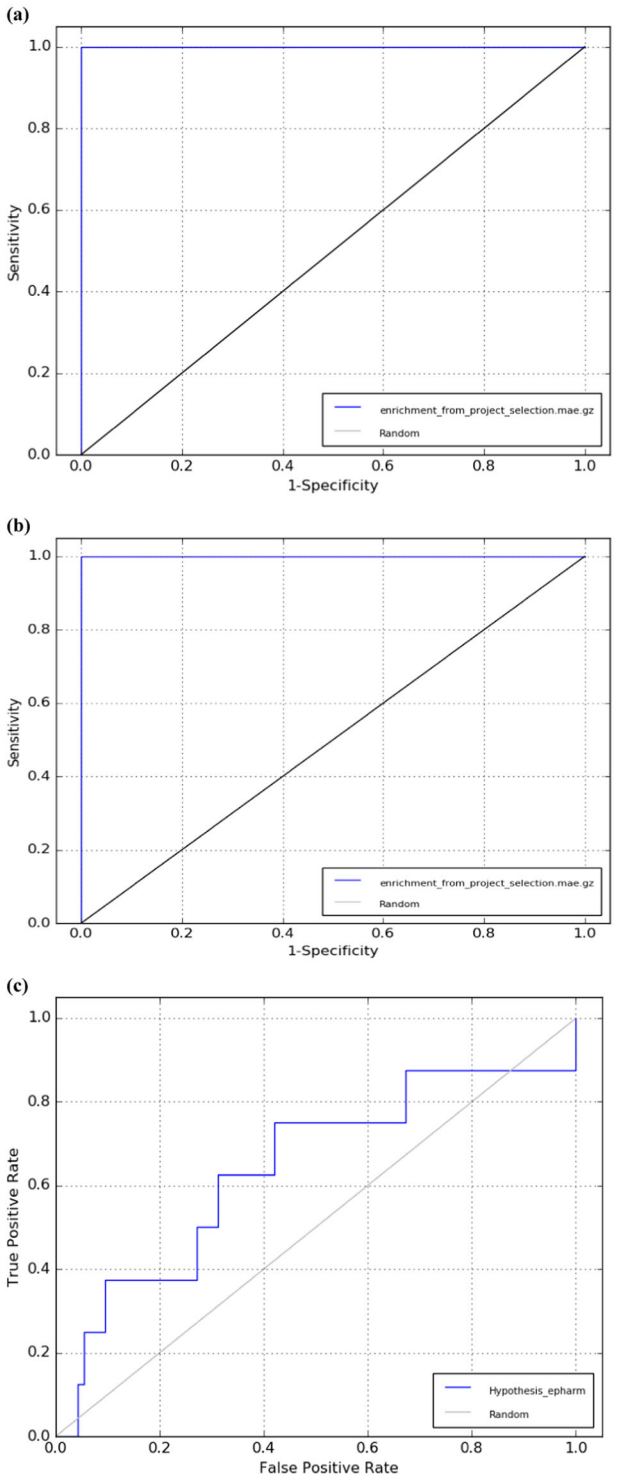

Fig. 3 Receiver operating characteristics curve (ROC) plot for **a** ligand based pharmacophore model, **b** e-pharmacophore model, and **c** receptor cavity based pharmacophore model

This shows that the models are able to rank the actives effectively at the beginning of the screening process [33]. The ROC value of 1 also depicts that the models have a chance of screening actives 100% effectively from decoy set. The ROC value of 0.649 for receptor cavity based pharmacophore model implies that the model has comparatively less ability to screen actives in the beginning (Fig. 3c). These results suggest that combining the results of these models would certainly outperform the current strategies.

Shape Screening

In shape-based screening, each conformer of molecules was aligned on the query ligand and a similarity was calculated based on hard-sphere volumes [20]. The NAI, oseltamivir, was used as the query ligand for shape screening against the database. The compounds recovered from the screen were further sorted using the shape similarity score (Shape_sim). Molecules possessing a similarity score more than 0.5 were subjected to docking analysis. In our study, a total number of 142 molecules possess match score of greater than threshold, 0.5. These molecules were then carried forward for further analysis.

Molecular Docking

Initially, the strength and direction of the linear relationships between pairs of variables such as IC50 and docking energy are studied by means of Pearson's correlation coefficients. The coefficient of 0.8321 resulted in our analysis highlights the strong prediction accuracy of glide algorithm for NA protein set. Thus, Schrödinger Suite's Glide module was used to execute molecular docking. Initially, PHASE search was performed with all the generated hypotheses. A total of 1000 molecules were retrieved as the matches for each hypothesis. These compounds together with 142 hits from shape screening were considered for docking analysis. The hits were ranked using multiple docking procedures viz HTVS, SP, and XP. The docking score of oseltamivir was used as the reference to screen the molecules in all the categories. For instance, ligand-based pharmacophore approach and receptor cavity based approach resulted in five hits, whereas the e-pharmacophore approach and shape screening resulted in six hits. Table 1 depicts the docking scores of all the hits. The resultant docking hits from each hypothesis were compared with figure out the common occurrence. It is interesting to note that out of four methodologies, three methods namely ligand-based pharmacophore modeling, e-pharmacophore modeling, and shape screening have resulted in a common hit, alprostadil (DB00770) for NA inhibition with binding affinity of −7.649 kcal/mol. It is to be noted that the hit DB00770 was not yielded by the receptor cavity based technique. This is consistent with the data that among the implemented algorithm receptor cavity method correlates to low selectivity and specificity.

Table 1 Glide scores and energy involvement of oseltamivir and screened hit molecules

S. No.	Hit compounds	Glide energy (kcal/mol)	Docking score (kcal/mol)
1.	Oseltamivir (DB00198)	−42.387	−4.882
Pharmacophore-based virtual screening			
2.	DB00770[a]	−71.531	−7.108
3.	DB00722	−70.531	−7.108
4.	DB00610	−57.863	−7.065
5.	DB00193	−61.331	−7.041
6.	DB00905	−61.331	−7.041
E-pharmacophore-based virtual screening			
7.	DB00171	−75.607	−9.002
8.	DB00770[a]	−68.321	−7.854
9.	DB01082	−45.387	−6.563
10.	DB06441	−66.076	−5.549
11.	DB00686	−57.607	−5.463
12.	DB09050	−62.461	−4.906
Receptor cavity based virtual screening			
13.	DB00355	−49.56	−7.057
14.	DB03147	−66.86	−6.818
15.	DB11596	−66.267	−6.199
16.	DB09050	−77.623	−5.984
17.	DB00179	−37.665	−4.945
Shape-based screening			
18.	DB00581	−43.184	−8.799
19.	DB00558	−37.899	−7.723
20.	DB00770[a]	−48.218	−7.01
21.	DB06614	−40.096	−6.549
22.	DB01203	−46.949	−6.317
23.	DB04573	−37.315	−5.529

[a]Hit molecule occurring in common among the studies

Furthermore, the interaction profile and ADME properties of the molecule were analyzed to gain insight into the binding pattern and pharmacokinetic properties.

Interaction Profile and ADME Analysis of Hit Compound

The hit compound was then further analysed to identify their best docking pose. It revealed that the interaction profile of hit compound was similar to oseltamivir-NA. The interaction pattern of alprostadil-NA and oseltamivir-NA is portrayed in Fig. 4. Oseltamivir forms hydrogen bond interaction with catalytic residues such as R 292, R 371, E 119, and R 152. The amine group ($-NH_2$) of oseltamivir forms hydrogen bond with E 119 residue, while oxygen atom forms hydrogen bond with R 292, R 371, and R 152 residues. Similarly, the hit compound also formed hydrogen bond with key binding site residues such as E 119, R 371, R 292, and R 118. In addition, it was also observed that the interacting distances were found to be similar to that of oseltamivir's interacting distances (Table 2). Furthermore, the pharmacokinetic properties of the compound were examined Qikprop tool of Schrödinger Suite [36]. It is worth mentioning that our hit molecule has a #stars value of 0 and a CNS value −2 indicating that it has no violation to drug likeliness and no CNS activity. The ADME properties of hit and known inhibitors are illustrated in Table 3. The table depicts the similarities between the known inhibitor and the hit compound pharmacokinetic properties. Altogether, the interaction studies and ADME analysis highlight that the hit compound, alprostadil shared similar safety profile, and better binding score than oseltamivir.

Biological Activity Analysis using PASS Algorithm

Furthermore, to validate the results, the biological activity of the compound was predicted using PASS algorithm. The results are shown in Table 4. The table clearly shows that alprostadil is possessing antiviral activity against influenza virus, rhinovirus, herpes virus, CMV, picornavirus, and poxvirus. Of note it was specifically predicted to have antiviral activity against influenza A virus with a *Pa* value of 0.317. It was also observed that the *Pa* value is comparatively higher than the *Pi* value of each prediction.

It is evident from the literature that alprostadil is a naturally occurring prostaglandin also known as prostaglandin E1 (PGE1). Prostaglandins are known to maintain homeostatic functions and also arbitrate pathogenic mechanisms such as inflammatory response [42]. Of note prostaglandins are reported to possess antiviral activity against many DNA and RNA viruses [43]. Moreover the Δ^{12}-Prostaglandin J2 is known to exhibit therapeutic activity against influenza A virus (H1N1) both in in vitro and in vivo studies. This is because it interferes with the replication of virus at various stages. There are other types of prostaglandins, which are reportedly known to show antiviral activities against deadly viruses like vaccinia virus, sendai, and vesicular somatostatis virus, herpes simplex virus type 1, and encephalomayocaditis virus [44, 45]. In another instance, a study conducted at University of Science and Technology, China, the compound alprostadil was shown to have inhibitory activity against hepatitis virus infection [46].

Docking Analysis with NA Mutants

The hit molecule was also examined for its efficacy towards the NA mutant structures using XP docking algorithm. The mutant structures namely H274Y, R292K, E119G, N294S,

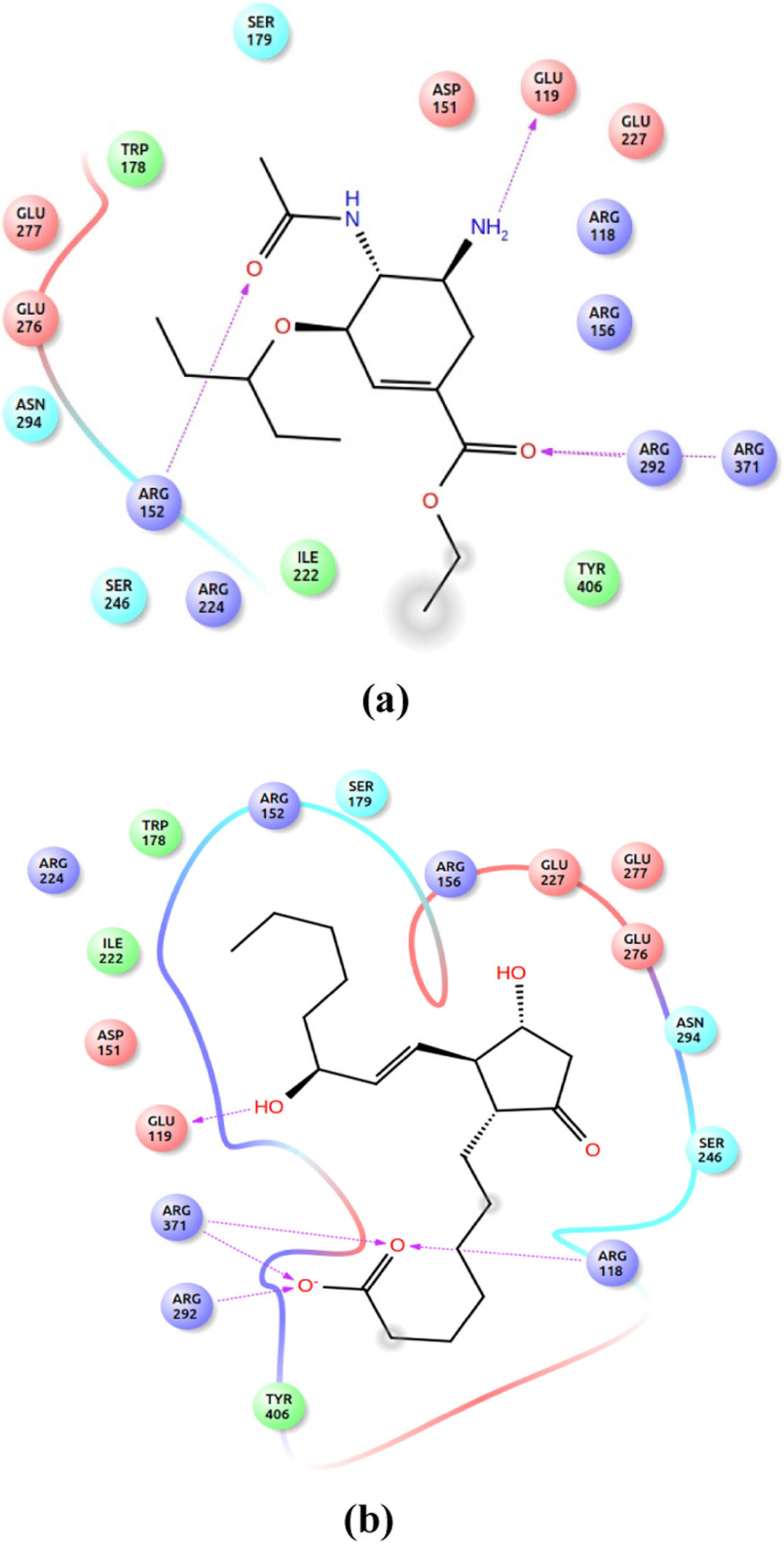

Fig. 4 2D interaction profiles of Neuraminidase with **a** oseltamivir (DB00198) and **b** alprostadil (DB00770). Hydrogen bond interactions with amino acids are represented in pink line. The interactions are shown with arrow head directing toward the electron donor

I223R, D179E, and I221L were investigated in our analysis. The results are shown in Table 5. It is clear from the table that the hit molecule exhibited better binding efficiency than oseltamivir. The glide scores of oseltamivir ranged from −3.329 to −4.644 kcal/mol, whereas in case of alprostadil the scores ranged from −4.592 to −5.637 kcal/mol. This

Table 2 Intermolecular interaction of alprostadil with neuraminidase protein

S. No.	Compounds	Number of H-bonds	Interacting atoms of protein-ligand complex	Distance (Å)
1.	Oseltamivir (DB00198)	4	Arg292…Lig(O)	2.3440
			Arg371…Lig(O)	1.8260
			Arg152…Lig(O)	2.1483
			Glu119…Lig(NH_2)	2.0835
2.	DB00770	5	Lig(O)… Arg 118	2.4908
			Arg371…Lig(O)	1.7410
			Arg371…Lig(O^-)	1.8030
			Lig(O^-)…Arg 292	2.5880
			Lig(OH)…Glu119	2.0721

clearly highlights the stable binding of alprostadil with all the studied NA mutant structures. Moreover the hit molecule was found to interact with key residues such as R 292, R 371, and R 152 in the NA structure. Thus, we assumed that the hydrogen bond interaction with these crucial residues could also be plausible for the stable binding of hit with the explored NA mutant structures.

MD Simulations

The MD simulation studies serve as a significant platform to gain an insight into protein-ligand binding mechanisms. Specifically, the parameters like RMSD, RMSF, and number of inter hydrogen bonds unequivocally help in determining the protein-ligand interaction pattern [47].

The RMSD values were computed to analyse the conformational changes and stability of protein-ligand complexes over the course of the trajectory. The results are shown in Fig. 5. Here, the RMSD trend for alprostadil-NA protein is represented in red color and the oseltamivir-NA protein in black color (the similar color coding scheme is adopted throughout the study). The figure clearly revealed similar fashion of deviations in backbone RMSD among the alprostadil-NA and oseltamivir-NA complexes till ~19 ns. However, RMSD trends in the later part of the simulation were found to deviate and stabilized at 30 ns with the value of ~0.26 nm for the hit compound. On the contrary, the oseltamivir-NA protein complex deviates more in the later part of the simulation and attain the high RMSD value of ~0.3 nm at 32 ns approximately. The RMSD value of both the complexes showed negligible variations between 30 and 50 ns indicating structural stabilization. Importantly, the lesser RMSD value of alprostadil-NA protein complex highlights the stable binding than oseltamivir-NA protein complex.

Furthermore, the RMSF calculations were carried out to characterize local changes along the protein chain. Figure 6 depicts the residue wise RMSF details of the protein-ligand complexes. The peaks in RMSF are the highly flexible region in the protein structure along the simulation. It is evident from the figure that the residues from 250th to 420th positions were showing higher fluctuations in case of oseltamivir-NA complex than alprostadil-NA system. This region specifically constitutes of vital binding site residues such as E 277, R 292, N 294, N 347, R 371, and Y 406. Thus signifies less involvement of these residues in the oseltamivir binding. On the other hand, the alprostadil-NA protein complex exhibited less fluctuation in the active site region suggesting that involvement of these key residues in the stable binding of alprostadil.

The intermolecular hydrogen bonds in the protein-ligand complexes were also monitored throughout the simulation period as these are relative measure of binding affinity. Figure 7 clearly shows that the hit compound, alprostadil is able to maintain an average of 4–5 hydrogen bonds throughout the simulation. At some places it was also found to maintain up to six hydrogen bond interactions. It is also noteworthy to mention that the alprostadil is maintaining five interactions as observed in interaction profile of alprostadil and NA protein complex. In contrast, oseltamivir exhibited an average of three hydrogen bonds in the course of simulation. The persistence of highest number of intermolecular interaction highlights the stable binding of alprostadil in the NA binding pocket.

In addition, the cluster analysis was performed using g_cluster utility to highlight the flexibility of the protein complexes. The statistics of the cluster analysis are shown in Table 6. It is evident from the table that NA protein complexed with oseltamivir showed less number of clusters when compared with NA and aplrostadil complex. It was also observed that the members were less in the most populated cluster of NA-alprostadil complex than NA-oseltamivir complex. These observations clearly signify that NA-alprostadil complex is more structurally flexible when compared with NA-oseltamivir complex. It is worth mentioning that similar trend was observed during structural and functional analysis of FUS gene reported in the recent literature [48]. An illustration of middle conformation

Table 3 Absorption, distribution, metabolism, and excretion (ADME) properties of reference drugs and screened hit molecule

Compounds[a]	mol MW[b]	SASA[c]	FOSA[d]	donorHB[e]	accptHB[f]	HOA[g]	QplogKp[h]	QplogBB[i]	QplogS[j]	QplogPo/w[k]	QplogPw[l]	QplogPoc[o]t[m]	#stars[n]	CNS
Crenatoside	622.579	864.446	272.216	8	20.3	1	−6.146	−4.304	−2.954	−1.4	34.231	41.753	8	−2
DHEA	288.429	529.744	407.379	1	3.7	3	−3.021	−0.272	−4.176	3.292	6.715	14.413	0	0
Laninamivir	346.339	602.263	227.621	8	12.35	1	−9.187	−3.506	−1.187	−2.254	27.48	28.907	5	−2
Zanamivir	332.313	581.266	183.932	9	12.35	1	−9.524	−3.671	−0.926	−2.757	29.127	29.613	6	−2
Oseltamivir	312.408	632.207	485.104	3	7.2	3	−5.195	−0.822	−1.79	0.985	13.935	18.523	0	−2
Peramivir	328.411	588.343	325.743	6	7.2	2	−7.558	−2.373	−1.997	0.315	18.428	23.269	0	−2
Tamiphosphor	320.325	559.233	334.481	5	10.2	1	−6.595	−1.437	−0.665	−2.211	19.907	22.137	1	−2
MK2206	407.474	695.999	140.51	3	5	3	−5.104	−1.061	−4.957	3.445	13.609	23.255	1	−2
Alprostadil	354.486	765.495	528.413	3	7.4	2	−4.224	−2.948	−3.713	3.029	11.548	21.187	0	−2

[a]Ligand IDs for the ZINC database

[b]Molecular weight

[c]Solvent accessible surface area

[d]Hydrophobic solvent accessible surface area

[e]Hydrogen Bond donor

[f]Hydrogen Bond acceptor

[g]Predicted percentage of human oral absorption

[h]Predicted skin permeability

[i]Predicted brain/blood partition coefficient

[j]Predicted aqueous solubility

[k]Predicted water/octanol partition coeffient

[l]Predicted water/gas partition coefficient

[m]Predicted octanol/gas partition coefficient

[n]Number of property or descriptor values that fall outside the 95% range of similar values for known drugs

[o] Predicted central nervous system activity on a −2 (inactive) to +2 (active) scale

Table 4 Biological activity prediction of alprostadil using PASS algorithm

Pa	*Pi*	Activity
0.692	0.006	Antiviral (Influenza)
0.595	0.007	Antiviral (Rhinovirus)
0.399	0.036	Antiviral (Herpes)
0.317	0.031	Antiviral (Influenza A)
0.305	0.027	Antiviral (CMV)
0.330	0.183	Antiviral (Picornavirus)
0.222	0.128	Antiviral (Poxvirus)

Table 5 Glide score of hit molecule with NNA mutant structure

S. No.	Protein	Glide score (kcal/mol)	
		Oseltamivir	Alprostadil
1.	Native NA	−4.882	−7.100
2.	D179E	−3.761	−5.140
3.	E119G	−4.069	−4.832
4.	H274Y	−4.644	−5.637
5.	I221L	−4.389	−4.592
6.	I223R	−3.329	−5.017
7.	N294S	−4.335	−4.973
8.	R292K	−4.252	−4.844

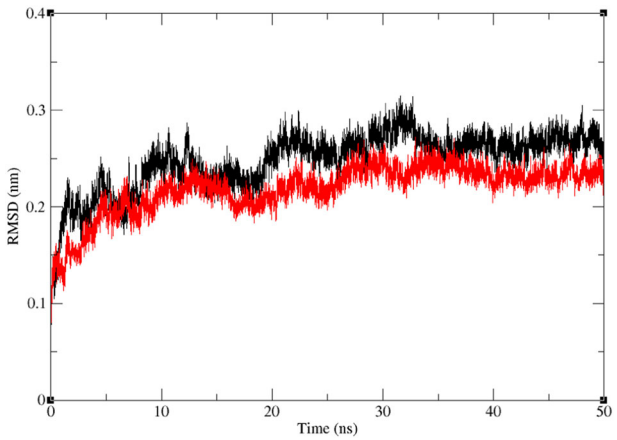

Fig. 5 Root mean square deviation corresponding to oseltamivir-NA protein complex (black) and alprostadil-NA protein complex (red) along the MD simulation at 300 K temperature and 1.01325 bar pressure

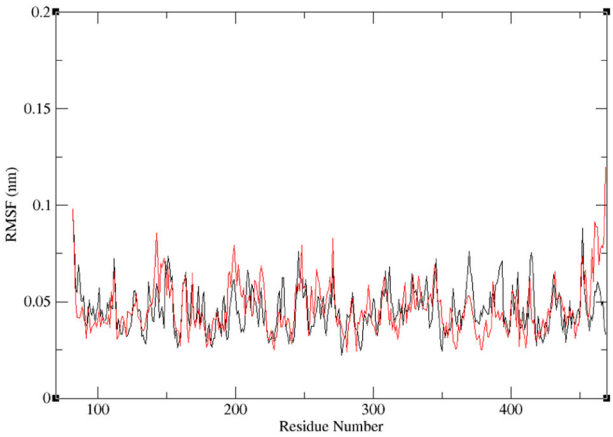

Fig. 6 Root mean square fluctuation of each residue averaged over the duration of the MD simulation

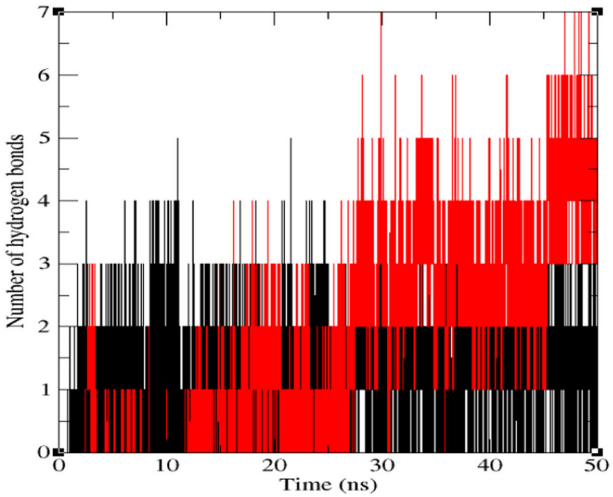

Fig. 7 Total number of intermolecular hydrogen bond exhibited in oseltamivir-NA complex (black) and alprostadil-NA protein complex (red) throughout the simulation

Table 6 Statistics of clustering analysis of NA-oseltamivir and NA–alprostadil complexes obtained from MD trajectories

Protein complex	Total number of clusters	Total number of members in most populated cluster
NA-Oseltamivir	15	12946
NA-Alprostadil	17	12507

representing the average structure of each cluster of both the complexes is shown in Fig. 8.

Finally, the binding pocket of the protein complexes was analysed using the SiteMap module. The final MD trajectories of each complex were split into six PDB files from 0 to 50 ns with intervals of 10 ns. These PDB files were then subjected to SiteMap analysis to evaluate the Dscore or druggability score, enclosure value, and site score. The results are shown in Table 7. It is clear from the table that the Dscores of all the PDB files of protein complexes at various time frames were >0.8. Thus, highlights that the protein binding pockets at each time frame prove to be druggable [49]. Moreover the site score and enclosure values of the proteins were also observed to be greater than 0.88 and 0.78, respectively. These scores suggest that the pockets are deep and more enclosed. This consecutively proves that the pockets are more hydrophobic in nature and

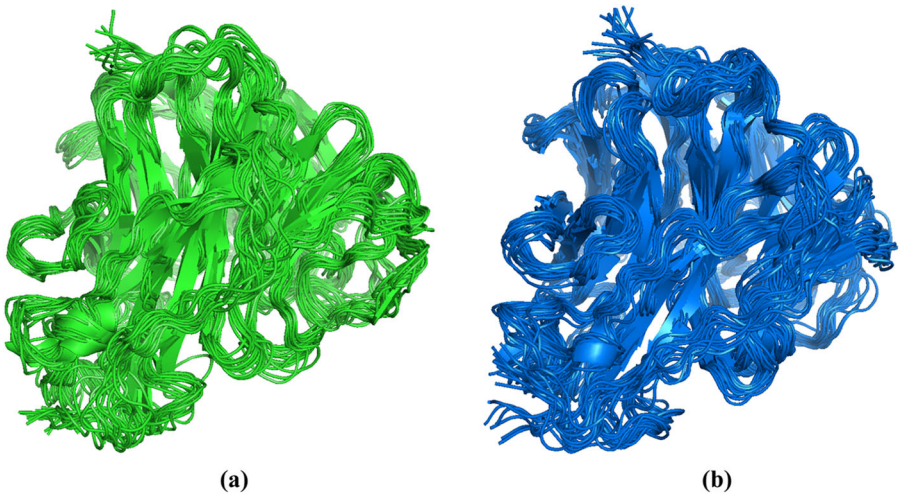

Fig. 8 Representation of middle conformation showing the average structure of each cluster of **a** NA protein-oseltamivir complex and **b** NA protein-alprostadil complex

Table 7 SiteMap parameters of PDB files of protein complexes at different time frames

Protein complex PDB files at different time frames	SiteMap parameters	Oseltamivr	Aprostadil
Protein 0 (0 ns)	D score	0.970	0.975
	Site score	1.055	1.056
	Enclosure	0.781	0.781
Protein 1 (0–10 ns)	D score	0.907	0.884
	Site score	1.063	0.772
	Enclosure	0.792	0.780
Protein 2 (10–20 ns)	D score	0.873	0.824
	Site score	0.887	0.763
	Enclosure	0.785	0.799
Protein 3 (20–30 ns)	D score	0.887	0.982
	Site score	0.983	1.024
	Enclosure	0.790	0.784
Protein 4 (30–40 ns)	D score	0.956	0.835
	Site score	1.033	0.890
	Enclosure	0.788	0.781
Protein 5 (40–50 ns)	D score	0.999	0.800
	Site score	1.012	0.869
	Enclosure	0.797	0.848

eventually aids in achieving adequate binding affinity with drug like compound [49]. Therefore, it can be implied from these parameters that the binding pockets at each time frame of both the complexes are highly druggable.

Conclusion

The influenza epidemics have never revealed any conventional pattern or periodicity. Moreover, the emergence of novel mutations in influenza virus has augmented resistance to the existing NAI. Thus, it is high time to discover efficient inhibitor for the treatment of influenza. Computational methods that can assist polypharmacology are of key importance in drug development. Here, we introduced an integrated approach that incorporates the concepts of ligand-, energy-, receptor cavity-, and shape based pharmacophore hypothesis for making the recommendations of the hit molecules. The hypothesis built from the available drug compounds showed excellent statistical significance by enrichment calculation. Further multiple docking strategy viz HTVS, SP, and XP algorithm enabled us to achieve the binding affinity data analysis of hit compounds against NA.

These analyses revealed that among the available drugs in our dataset, the best docking energy was exhibited by alprostadil with binding affinity of −7.649 kcal/mol. In essence, significant Pearson's correlation coefficient of 0.8051 observed between the approved molecule and its IC50 values highlights that glide docking algorithm could discriminate non binders from active compounds with more than 80% predictive accuracy. Drugs scans analysis performed by Qikprop and PASS algorithm were evident that alprostadil possess better pharmacokinetic and dynamics properties than oseltamivir. Finally, mutation studies and MD simulation on alprostadil are also encouraging than the oseltamivir in terms of stability and kinetics of binding with NA. Overall, we conclude that Alprostadil portrays the desirable qualities to be a potent anti-viral drug, which could be repurposed for influenza treatment in the near future.

Acknowledgements The authors gratefully acknowledge Vellore Institute of Technology, Vellore for the support through Seed Grant for Research. V.S. acknowledges support from Bioinformatics Resources and Applications Facility (BRAF), C-DAC, Pune. K.R. also thank to ICMR for their support by the International Fellowship for Young Biomedical Scientists Award.

Compliance with Ethical Standards

Conflict of Interest The authors declare that they have no conflict of interest.

Publisher's note Springer Nature remains neutral with regard to jurisdictional claims in published maps and institutional affiliations.

References

1. Jagadesh, A., Salam, A. A. A., Mudgal, P. P., & Arunkumar, G. (2016). Influenza virus neuraminidase (NA): a target for antivirals and vaccines. *Archives of Virology*, *161*, 2087–2094.
2. Wang, M. Z., Tai, C. Y., & Mendel, D. B. (2002). Mechanism by which mutations at His274 alter sensitivity of influenza A virus N1 neuraminidase to oseltamivir carboxylate and zanamivir. *Antimicrobial Agents and Chemotherapy*, *46*, 3809–3816.
3. Loveday, E. K., Diederich, S., Pasick, J., & Jean, F. (2015). Human microRNA-24 modulates highly pathogenic avian-origin H5N1 influenza A virus infection in A549 cells by targeting secretory pathway furin. *Journal of General Virology*, *96*, 30–39.
4. Li, Y., Lin, Z., Zhao, M., Guo, M., Xu, T., Wang, C., Xia, H., & Zhu, B. (2016). Reversal of H1N1 influenza virus-induced apoptosis by silver nanoparticles functionalized with amantadine. *RSC Advances*, *6*, 89679–89686.
5. Bauer, K., Richter, M., Wutzler, P., & Schmidtke, M. (2009). Different neuraminidase inhibitor susceptibilities of human H1N1, H1N2, and H3N2 influenza A viruses isolated in Germany from 2001 to 2005/06. *Antiviral Research*, *82*, 34–41.
6. Hurt, A. C., Holien, J. K., Parker, M., & Barr, I. G. (2009). Oseltamivir resistance and the H274Y neuraminidase mutation in seasonal, pandemic and highly pathogenic influenza viruses. *Drugs*, *69*, 2523–2531.
7. Shobugawa, Y., Saito, R., Sato, I., Kawashima, T., Dapat, C., Dapat, I. C., Kondo, H., Suzuki, Y., Saito, K., & Suzuki, H. (2012). Clinical effectiveness of neuraminidase inhibitor—oseltamivir, zanamivir, laninamivir, and peramivir—for treatment of influenza A(H3N2) and A(H1N1) pdm09 infection: an observational study in the 2010–2011 influenza season in Japan. *Journal of Infection and Chemotherapy*, *18*, 858–864.
8. Wu, N. C., Young, A. P., Dandekar, S., Wijersuriya, H., Al-Mawsawi, L. Q., Wu, T. T., & Sun, R. (2013). Systematic identification of H274Y compensatory mutations in influenza A virus neuraminidase by high-throughput screening. *Journal of Virology*, *87*, 1193–1199.
9. Yen, H. L., McKimm-Breschkin, J. L., Choy, K. T., Wong, D. D. Y., Cheung, P. P. H., Zhou, J., Ng, I. H., Zhu, H., Webby, R. J., Guan, Y., Webster, R. G., & Peirisa, J. S. M. (2013). Resistance to neuraminidase inhibitors conferred by an R292K mutation in a human influenza virus H7N9 isolate can be masked by a mixed R/ K viral population. *MBio*, *4*, e00396–13.
10. McKimm-Breschkin, J. L. (2012). Influenza neuraminidase inhibitors: antiviral action and mechanisms of resistance. *Influenza and Other Respiratory Viruses*, *7*, 25–36.
11. Escuret, V., Collins, P. J., Casalegno, J. S., Vachieri, S. G., Cattle, N., Ferraris, O., Sabatier, M., Frobert, E., Caro, V., Skehel, J. J., Gamblin, S., Valla, F., Valette, M., Ottmann, M., McCauley, J. W., Daniels, R. S., & Lina, B. (2014). A novel I221L substitution in neuraminidase confers high-level resistance to oseltamivir in influenza B viruses. *Journal of Infectious Diseases*, *210*, 1260–1269.
12. LeGoff, J., Rousset, D., Abou-Jaoudé, G., Scemla, A., Ribaud, P., Mercier-Delarue, S., Caro, V., Enouf, V., Simon, F., Molina, J., & van der Werf, S. (2012). I223R mutation in influenza A(H1N1) pdm09 neuraminidase confers reduced susceptibility to oseltamivir and zanamivir and enhanced resistance with H275Y. *PLoS ONE*, *7*, e37095.
13. Li, J., Zheng, S., Chen, B., Butte, A. J., Swamidass, S. J., & Lu, Z. (2015). A survey of current trends in computational drug repositioning. *Briefings in Bioinformatics*, *17*, 2–12.
14. Shaughnessy, A. F. (2011). Old drugs, new tricks. *BMJ*, *342*, d741.
15. Moonsamy, S., Bhakat, S., Ramesh, M., & Soliman, M. E. (2017). Identification of binding mode and prospective structural features of novel nef protein inhibitors as potential anti-HIV drugs. *Cell Biochemistry and Biophysics*, *75*, 49–64.
16. Karthick, V., Shanthi, V., Rajasekaran, R., & Ramanathan, K. (2013). In silico analysis of drug-resistant mutant of neuraminidase (N294S) against oseltamivir. *Protoplasma*, *250*, 197–207.
17. James, N., & Ramanathan, K. (2018). Discovery of potent ALK inhibitors using pharmacophore-informatics strategy. *Cell Biochemistry and Biophysics*, *76*, 111–124.
18. Rohini, K., & Shanthi, V. (2018). Hyphenated 3D-QSAR statistical model-drug repurposing analysis for the identification of potent neuraminidase inhibitor. *Cell Biochemistry and Biophysics*, *76*, 357–376.
19. Karthick, V., & Ramanathan, K. (2014). Computational investigation of drug-resistant mutant of M2 proton channel (S31N) against rimantadine. *Cell Biochemistry and Bbiophysics*, *70*, 975–982.
20. Karthick, V., Ramanathan, K., Shanthi, V., & Rajasekaran, R. (2013). Identification of potential inhibitors of H5N1 influenza A virus neuraminidase by ligand-based virtual screening approach. *Cell Biochemistry and Biophysics*, *66*, 657–669.
21. Berman, H. M., Westbrook, J., Feng, Z., Gilliland, G., Bhat, T. N., & Weissig, H. (2000). The protein data bank. *Nucleic Acids Research*, *28*, 235–242.
22. Vavricka, C. J., Li, Q., Wu, Y., Qi, J., Wang, M., Liu, Y., Gao, F., Liu, J., Feng, E., He, J., Wang, J., Liu, H., Jiang, H., & Gao, G. F. (2011). Structural and functional analysis of laninamivir and its octanoate prodrug reveals group specific mechanisms for influenza NA inhibition. *PLoS Pathogens*, *7*, e1002249.
23. Ramar, V., & Pappu, S. (2016). Exploring the inhibitory potential of bioactive compound from Luffa acutangula against NF-κB-A molecular docking and dynamics approach. *Computational Biology and Chemistry*, *62*, 29–35.
24. Aparna, V., Dineshkumar, K., Mohanalakshmi, N., Velmurugan, D., & Hopper, W. (2014). Identification of natural compound inhibitors for multidrug efflux pumps of Escherichia coli and Pseudomonas aeruginosa using in silico high-throughput virtual screening and in vitro validation. *PLoS ONE*, *9*, e101840.
25. Vass, M., Schmidt, É., Horti, F., & Keserű, G. M. (2014). Virtual fragment screening on GPCRs: a case study on dopamine D3 and histamine H4 receptors. *European Journal of Medicinal Chemistry*, *77*, 38–46.
26. Bhadoriya, K. S., Sharma, M. C., & Jain, S. V. (2015). Pharmacophore modeling and atom-based 3D-QSAR studies on amino derivatives of indole as potent isoprenylcysteine carboxyl methyltransferase (Icmt) inhibitors. *Journal of Molecular Structure*, *1081*, 466–476.
27. Watts, K. S., Dalal, P., Murphy, R. B., Sherman, W., Friesner, R. A., & Shelley, J. C. (2010). ConfGen: a conformational search method for efficient generation of bioactive conformers. *Journal of Chemical Information and Modeling*, *50*, 534–546.
28. Dixon, S. L., Smondyrev, A. M., & Rao, S. N. (2006). PHASE: a novel approach to pharmacophore modeling and 3D database searching. *Chemical Biology & Drug Design*, *67*, 370–372.

29. Carlson, H. A., Masukawa, K. M., & McCammon, J. A. (1999). Method for including the dynamic fluctuations of a protein in computer-aided drug design. *Journal of Physical Chemistry A*, *103*, 10213–10219.
30. Halgren, T. A., Murphy, R. B., Friesner, R. A., Beard, H. S., Frye, L. L., Pollard, W. T., & Banks, J. L. (2004). Glide: a new approach for rapid, accurate docking and scoring. 2. Enrichment factors in database screening. *Journal of Medicinal Chemistry*, *47*, 1750–1759.
31. Nair, S. B., Fayaz, S. M., & Krishnamurthy, R. G. (2012). In silico prediction of novel inhibitors of the DNA binding activity of FoxG1. *Medicinal Chemistry*, *8*, 1155–1162.
32. Mysinger, M. M., Carchia, M., Irwin, J. J., & Shoichet, B. K. (2012). Directory of useful decoys, enhanced (DUD-E): better ligands and decoys for better benchmarking. *Journal of Medicinal Chemistry*, *55*, 6582–6594.
33. Truchon, J. F., & Bayly, C. I. (2007). Evaluating virtual screening methods: good and bad metrics for the "early recognition" problem. *Journal of Chemical Information and Modeling*, *47*, 488–508.
34. Rohini, K., & Shanthi, V. (2018). Discovery of potent neuraminidase inhibitors using a combination of pharmacophore-based virtual screening and molecular simulation approach. *Applied Biochemistry and Biotechnology*, *184*, 1421–1440.
35. Kumar, N., & Pruthi, V. (2015). Structural elucidation and molecular docking of ferulic acid from Parthenium hysterophorus possessing COX-2 inhibition activity. *3 Biotech*, *5*, 541.
36. Lipinski, C. A. (2004). Lead- and drug-like compounds: the rule-of-five revolution. *Drug Discovery Today: Technologies*, *1*, 337–341.
37. Goel, R. K., Singh, D., Lagunin, A., & Poroikov, V. (2011). PASS-assisted exploration of new therapeutic potential of natural products. *Medicinal Chemistry Research*, *20*, 1509–1514.
38. Hess, B., Kutzner, C., Van Der Spoel, D., & Lindahl, E. (2008). GROMACS 4: algorithms for highly efficient, load-balanced, and scalable molecular simulation. *Journal of Chemical Theory and Computation*, *4*, 435–447.
39. Schuttelkopf, A. W., & Van Aalten, D. M. F. (2004). PRODRG—a tool for high-throughput crystallography of protein–ligand complexes. *Acta Crystallographica*, *60*, 1355–1363.
40. Van Der Spoel, D., Lindahl, E., Hess, B., Groenhof, G., Mark, A. E., & Berendsen, H. J. (2005). GROMACS: fast, flexible, and free. *Journal of Computational Chemistry*, *26*, 1701–1718.
41. Therese, P. J., Manvar, D., Kondepudi, S., Battu, M. B., Sriram, D., Basu, A., Yogeeswari, P., & Kaushik-Basu, N. (2014). Multiple e-pharmacophore modeling, 3D-QSAR, and high-throughput virtual screening of hepatitis C virus NS5B polymerase inhibitors. *Journal of Chemical Information and Modeling*, *54*, 539–552.
42. Pica, F., Palamara, A. T., Rossi, A., Marco, A. D., Amici, C., & Santoro, M. G. (2000). Δ^{12}- Prostaglandin J2 Is a Potent Inhibitor of Influenza A Virus Replication. *Antimicrobial Agents and Chemotherapy*, *44*, 200–204.
43. Burlandy, F. M., & Rebello, M. A. (2001). Inhibition of mayaro virus replication by prostaglandin A1 in vero cells. *Intervirology*, *44*, 344–349.
44. Ankel, H., Mittnacht, S., & Jacobsen, H. (1985). Antiviral activity of prostaglandin A on encephalomyocarditis virus-infected cells: a unique effect unrelated to interferon. *Journal of General Virology*, *66*, 2355–2364.
45. O'Brien, W. J., Taylor, J. L., Ankel, H., & Sitenga, G. (1996). Assessment of antiviral activity, efficacy, and toxicity of prostaglandin A2 in a rabbit model of herpetic keratitis. *Antimicrobial Agents and Chemotherapy*, *40*, 2327–2331.
46. Hui, C. H. (2003). Alprostadil in the treatment of 42 patients with severe viral hepatitis. *Herald of Medicine*, *4*, 10.
47. Sargsyan, K., Grauffel, C., & Lim, C. (2017). How molecular size impacts RMSD applications in molecular dynamics simulations. *Journal of Chemical Theory and Computation*, *13*, 1518–1524.
48. Kamaraj, B., Rajendran, V., Sethumadhavan, R., Kumar, C. V., & Purohit, R. (2015). Mutational analysis of FUS gene and its structural and functional role in amyotrophic lateral sclerosis 6. *Journal of Biomolecular Structure and Dynamics*, *33*, 834–844.
49. Halgren, T. A. (2009). Identifying and characterizing binding sites and assessing druggability. *Journal of Chemical Information and Modeling*, *49*, 377–389.